ASSOCIAZIONE NAZIONALE ITALIANA DI INGEGNERIA SISMICA
ANIDIS
Italian National Association of Earthquake Engineering

XVIII CONVEGNO ANIDIS
L'ingegneria sismica in Italia
ASCOLI PICENO 2019
15-19 Settembre

Recursive identification of frequency-amplitude model for damage detection in structures with non-linear behaviour

Said Quqa[a], Luca Landi[a], Pier Paolo Diotallevi[a]
[a] *Department of Civil, Chemical, Environmental, and Materials Engineering (DICAM), University of Bologna, Viale del Risorgimento 2, 40136 Bologna, Italy*

Keywords: Damage detection; non-linearity; non-stationarity; operational modal analysis

ABSTRACT
Most damage identification methods used in the field of structural health monitoring are based on comparing the modal parameters estimated at different time intervals. Since natural frequencies can be evaluated even by using limited instrumentation and does not require any signal synchronization procedure, frequency-based identification methods are of great interest for applications in real-time monitoring by means of low-cost sensing systems. In the last decades, several damage-sensitive features have been proposed in order to conduct damage identification minimizing the occurrence of errors under varying environmental conditions. However, the amplitude of input excitation can also lead to short-term frequency variations, due to a non-linear behaviour of civil structures. This paper proposes a procedure aimed at damage detection in non-linear structures based on frequencies and amplitudes of modal responses, estimated assuming a locally-linear structural behaviour. It is shown that, by analysing a set of instantaneous parameters, it is possible limit the problems related to an incorrect identification of the structural state of health when the effects of non-linearities on modal parameters prevail over those of an actual state of damage. The method proposed is applied to a set of data recorded on a reinforced concrete structure with strongly non-linear behaviour.

1 INTRODUCTION

To date, due to the advantages obtained also in economic terms, the growing importance of structural health monitoring is leading a large number of researchers to study versatile and precise methods, applicable not only to structures of strategic and monumental importance, but also to minor buildings and infrastructures, which however require constant control (Cardoso et al., 2019; Limongelli et al., 2019; Bazzucchi et al., 2018).

Because of their direct physical interpretation and efficiency achieved through the large number of computational algorithms proposed in the last decades, modal parameters (i.e., natural frequencies, modal shapes and damping) are among the most used for damage identification (Brinker and Ventura 2015). In particular, a variation of quantities calculated using modal parameters generally indicates a change in the structural dynamic behaviour and is often associated with ongoing damage. These quantities are therefore called damage-sensitive features (DSFs).

Recently, several monitoring solutions were proposed which employ Micro Electro-Mechanical System (MEMS) sensors combined with low-cost microcontrollers and wireless transmission modules, with less impact from the visual and economic point of view with respect to the traditional configurations based on wired piezoelectric sensors (Noel et al. 2017). Moreover, thanks to the computational capacity of microcontrollers, part of processing activities can be performed directly on board, in a decentralized topology. The issue of energy efficiency is of the utmost importance for low-cost solutions, since it is strictly related to the wireless transmission rate (Tokognon et al. 2017). Moreover, because of the lack of a centralized time reference, data synchronization is a critical issue when dealing with complex monitoring networks (Kim et al. 2016).

Since natural frequencies can even be estimated by means of a single sensor without requiring synchronization of acquired data, frequency-based

identification methods are particularly suitable for decentralized monitoring systems.

Although modal parameters are evaluated using linear models, civil structures generally exhibit different forms of non-linearity (Worden and Tomlinson 2001). This fact is usually neglected in traditional identification methods, assuming that signals on which modal analysis is performed are collected under low-intensity excitation and stationary environmental conditions, which include temperature, humidity, and the characteristics related to the input excitation (e.g., amplitude and frequency content). However, depending on the construction technology, some structures may reveal their non-linear behaviour even under ambient vibration, which is always present during operating conditions. Moreover, environmental effects are not always assumable as stationary and may therefore compromise the quality of identification results (Gentile et al, 2019; Zonno et al., 2019; Saisi et al. 2018; Giordano et al. 2018; Magalhães et al., 2012; Ramos et al., 2010; Peeters et al, 2001). A direct comparison of modal parameters obtained during different time intervals may therefore be misleading for the identification of damage, since the differences of estimated parameters could also be due to a variation of the exciting input or to environmental effects. In the last decades, several techniques for removing environmental effects from damage-sensitive features were proposed (Gentile et al. 2019). In addition, an increasing amount of methods to also consider structural non-linearities were developed (Billings 2013), most of which are computationally expensive and require a large amount of data, making them unsuitable for decentralized low-cost monitoring systems.

In this paper, we propose a data preparation criterion and a DSF which also takes into account the non-linearity of structural dynamic behaviour in a simple way. The DSF is based on the instantaneous frequency and amplitude of a selected modal response, extracted by means of an algorithm presented in a previous work (Quqa et al. 2019). The procedure is particularly suitable for applications with non-stationary or non-persistent input excitation. In order to show this fact, the method proposed is applied on accelerometric data collected during an experimental campaign conducted on a full-scale 7-story slice of a reinforced concrete building, tested with different excitation levels and in progressive induced damage conditions (Moaveni et al. 2010).

2 PROCEDURE OUTLINE

The identification algorithm used for the extraction of modal responses (Quqa et al. 2019) consists of a first initialization phase which involves the construction of a wavelet filter bank used to decompose the acquired signal into separate modal responses, and a real-time processing phase which lies in the estimation of instantaneous frequencies and amplitudes using the Teager Energy Operator (TEO). The estimation of instantaneous parameters is carried out assuming a local linear model. This method is also valid under the assumption of non-stationary signals.

In the case of low-cost monitoring solutions based on embedded systems, the storage space dedicated to identified instantaneous parameters should be reduced as much as possible, due to the limited capacity of low-cost electronic devices. However, the excitation characteristics may vary over time, resulting in a variation of the identified modal parameters, which may lead to an incorrect estimation of structural damage. It is therefore necessary to use a model consisting of a few parameters which describes the structural dynamic behaviour under a large set of different conditions, even those occurred a long time before the instant in which the structural state of health is evaluated. For this reason, the first step of the procedure proposed in this paper concerns a recursive selection of instantaneous identified parameters.

2.1 Data selection

First, at time instant $t = 0$, consider two zero-valued sequences $\varphi_0[n]$ and $\psi_0[n]$ with $1 < n < N$. Up to time instant $t = N$, replace $\varphi_0[t] = a[t]$ and $\psi_0[t] = f[t]$, where $a[t]$ and $f[t]$ are the instantaneous amplitude and frequency values respectively, estimated through the identification algorithm. Reorder than both the sequences in order of amplitude (e.g., such that $\varphi_0[n] < \varphi_0[n+1]$), obtaining $\varphi_t[n]$ and $\psi_t[n]$. At time instant $t = N + 1$, replace the terms $\varphi_t[p] = a[t]$ and $\psi_t[p] = f[t]$ with p such that:

$$|\varphi_t[p] - a[t]| \leq |\varphi_t[n] - a[t]| \; \forall n \in [1, N] \quad (1)$$

In this way, each couple of instantaneous parameters $(f, a)[t]$ replaces the terms with more similar amplitude in $\varphi_t[n]$ and $\psi_t[n]$. In particular, if the signal analysed has non-stationary amplitude, a large part of the data sequences is updated. On the other hand, if the signal is stationary, a small portion of data is updated, without losing the parts referred to different amplitude ranges.

2.2 *Model identification*

Following the updating procedure of frequency-amplitude data, at user-defined time intervals $\tau = r\Delta t$ with $r \in \mathbb{N}$, the ordered sequence $\psi_\tau[n]$ is processed through a median filter in order to restrain the fluctuations of instantaneous estimates, obtaining the filtered sequence $\bar{\psi}_\tau[n]$. The couples $(\varphi_\tau, \bar{\psi}_\tau)[n]$ are then fitted using non-linear least squares to a model described by the equation

$$y(x) = \frac{m_\tau}{\omega\sqrt{2\pi}} e^{-\frac{(x-\xi)^2}{2\omega^2}} \int_{-\infty}^{\frac{\alpha}{\omega}(x-\xi)} \frac{1}{\sqrt{2\pi}} e^{-\frac{t^2}{2}} dt \quad (2)$$

which represents the skew-normal distribution (Azzalini 2013), multiplied by a factor $m_\tau/2$, where m_τ is the mean value of $\varphi_\tau[n]$.

The identification can therefore be performed repeatedly, after updating the frequency-amplitude sequences, obtaining the recursive estimation of the model described in Equation 2, the parameters of which (i.e., ω, ξ, and α) can be employed to compute the instantaneous mean (μ), variance (σ^2) and skewness (γ) of the skew-normal distribution:

$$\mu = \xi + \omega\delta\sqrt{\frac{\pi}{2}} \quad (3)$$

$$\sigma^2 = \omega^2\left(1 - \frac{2\delta^2}{\pi}\right) \quad (4)$$

$$\gamma = \frac{4-\pi}{2} \frac{\left(\delta\sqrt{2/\pi}\right)^3}{(1-2\delta^2/\pi)^{3/2}} \quad (5)$$

$$\delta = \frac{\alpha}{\sqrt{1+\alpha^2}} \quad (6)$$

The damage-sensitive feature proposed in this paper takes into account these parameters and can be interpreted as an approximation of the mode of the distribution (Azzalini 2013) fitted to the data sequences obtained at time instant τ:

$$m_0[\tau] = \mu - \frac{\sigma\gamma}{2} \quad (7)$$

By comparing $m_0[\tau]$ with $\bar{m}_0$, computed as the median value of m_0 collected over a time interval referred to a baseline condition, a variation in the DSF can be associated with a modification of the structural dynamic behaviour and may be related to ongoing damage. In this work, the damage index is expressed as a percentage variation of $m_0[\tau]$ with respect to $\bar{m}_0$:

$$d[\tau] = \frac{m_0[\tau] - \bar{m}_0}{\bar{m}_0} \cdot 100 \quad (8)$$

It should be noted that, because of the data selection criterion, the algorithm is suitable even for non-persistently excited systems. Moreover, since the instantaneous identification of frequency and amplitude can be performed on board each sensing node, data transmissions can be limited to the cases in which the DSF exceeds a given threshold (i.e., when damage is detected). By comparing the results obtained from different devices, the robustness of this method may be increased.

3 APPLICATION

The case study analysed in this paper is a full-scale slice of a 7-story reinforced concrete building with cantilever structural walls acting as the lateral force resisting system, tested on a shaking table at the University of California, San Diego, through the George E. Brown Jr. Network for Earthquake Engineering Simulation program (Moaveni et al. 2010; Moaveni et al. 2011). The test structure (Figure 1) is 20 m high and is formed by two perpendicular walls in elevation (web and flange wall) and a concrete slab at each level. Furthermore, the structure has an auxiliary post-tensioned column which provides torsional stability and 4 gravity columns that support the slabs (Figure 2).

The shaking table tests have been designed to progressively damage the building through the simulation of four historical earthquakes of increasing intensity recorded in Southern California.

Figure 1. Test structure (Moaveni et al. 2010).

Before and after each test with seismic excitation, the building was subjected to white noise excitation of 0.03g root mean square (RMS) amplitude for 8 minutes and low amplitude ambient vibration for 3 minutes. In this report, only the acceleration collected in this "inspection" intervals of 11 minutes were used, merged together in a single set of data with a total duration of 3300 seconds. In particular, the first 11 minutes refer to a reference "undamaged" condition, after which the first seismic excitation (EQ1) of low-intensity was applied. EQ1 is the longitudinal component recorded from the Van Nuys station during the San Fernando earthquake of 1971. After the seismic excitation, another inspection interval of 11 minutes was analyzed. Subsequently, two intervals of the same length were recorded after two medium-intensity earthquakes (EQ2 and EQ3), taken as the transverse component recorded during the San Fernando earthquake from the Van Nuys station in 1971, and the longitudinal component of the Northridge earthquake recorded from the Woodland Hills Oxnard Boulevard station in 1994. The last inspection interval was recorded after a high-intensity 360° excitation (EQ4) recorded from the Sylmar Olive View Med during the Northridge earthquake of 1994.

The structure was instrumented with a dense network of sensors with a total of 45 channels: 29 longitudinal (three on each floor slab, one on the web wall at mid-height of each story, and one on the pedestal base), 14 transversal (2 on each floor slab), and 2 vertical (at the base, on the pedestal). The original data are sampled at 240 Hz. In this work, 7 acceleration channels have been used (i.e., only longitudinal data indicated in Figure 2), recorded at each floor level and downsampled at 100 Hz.

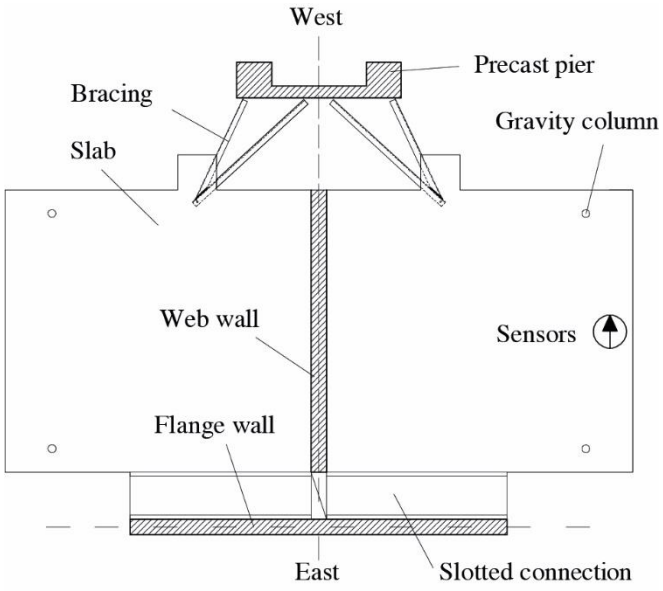

Figure 2. Floor scheme and location of sensors considered in this work (Martinelli et al. 2009).

The first step of the identification procedure was applied to a signal window of 60 seconds, collected under white noise excitation in the undamaged condition. The Fejér-Korovkin 14 wavelet function and a decomposition order 6 were selected in this phase. All the channels have been considered in the MAC-based clustering procedure. A threshold of 0.8 was chosen, and only consecutive components were assigned to the same cluster. In Figure 3 the filter bank obtained during the first step is reported, superimposed with the frequency spectra of each channel of the signal window used for initialization. The first mode has been selected, since its average energy value (represented as a black solid circle) is the only one above the threshold, computed as the mean of the energies of each cluster (black circles).

In the second step of the identification procedure, the entire set of recordings was processed through convolution with the selected bandpass filter. In this way, the modal response associated with the first vibration mode is extracted. Then, the instantaneous frequency and amplitude are evaluated by means of TEO. In this study, the analyses are performed offline. However, the algorithm allows the estimation of these quantities on board each sensor in real time, as new acceleration data is available, since only a short window of data is necessary for filtering and computing instantaneous parameters.

In Figure 4, a weighted average of the instantaneous frequencies computed at each node is represented, evaluated with respect to the instantaneous amplitudes. The overall amplitude, intended as the sum of instantaneous amplitudes evaluated considering the filtered signal of all nodes, is represented as a color scale in the same figure (the normalized values with respect to the maximum amplitude is reported).

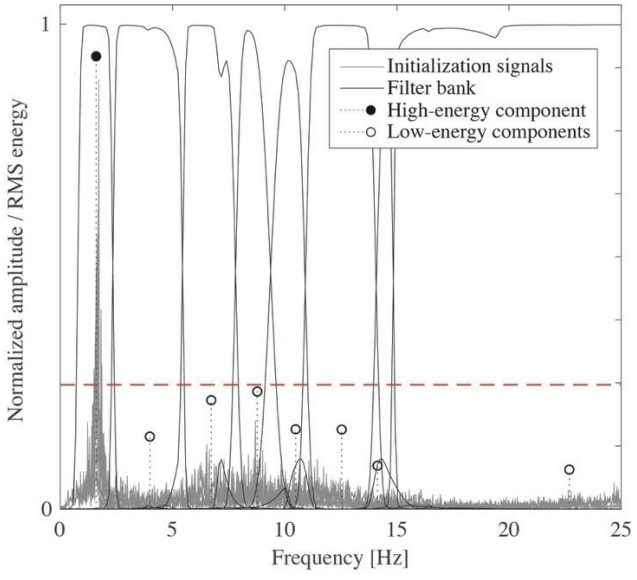

Figure 3. Filter bank for the extraction of modal response.

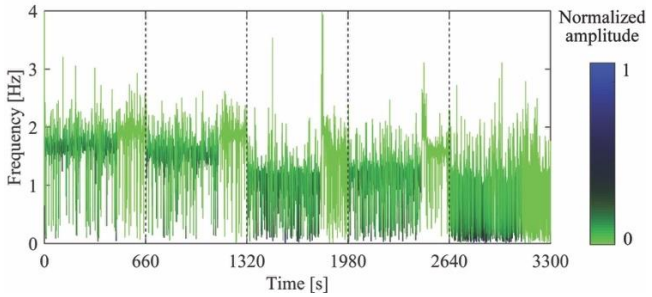

Figure 4. Average instantaneous frequency and amplitude (frequencies in ordinates and amplitudes as colour).

The dashed vertical lines in Figure 4 represent the limits between five different conditions: the interval from 0 to 660 seconds describes the structural behaviour in undamaged condition, while during the following intervals, data coming from progressively induced damage scenarios are used to compute the instantaneous frequency. Moreover, in the first part of each interval the acceleration recordings collected under 0.03g RMS white noise excitation are used, while, in the remaining part, the instantaneous frequency is evaluated under low-amplitude ambient vibration. This fact is also reflected in the plot colour, which is darker for larger response amplitude values (i.e., in the initial part of each damage scenario).

From Figure 4 it is possible to notice how the instantaneous frequency is particularly noisy and would need post-processing procedures (e.g. filtering) to be used as a damage-sensitive feature.

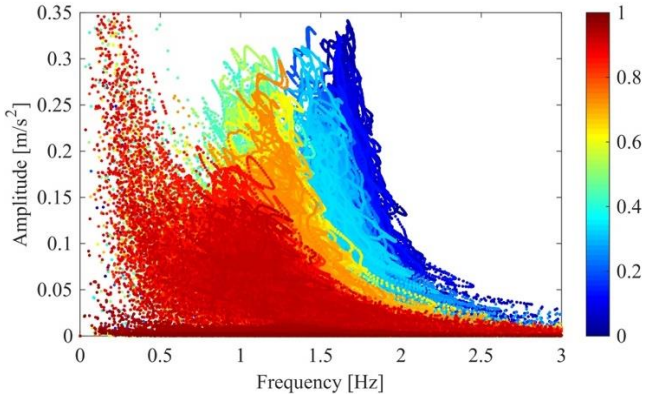

Figure 5. Original sets of identified parameters.

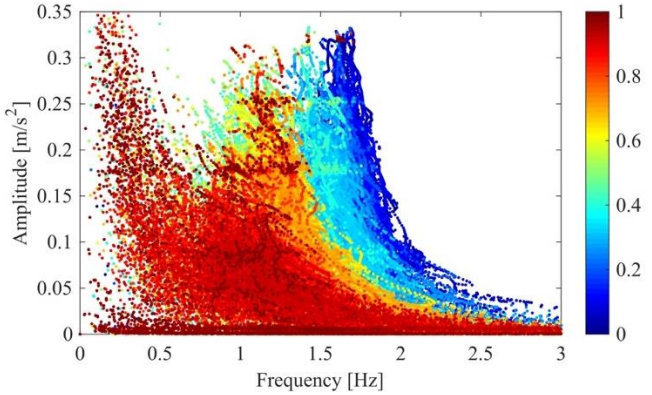

Figure 6. Reorganized sets of identified parameters.

Furthermore, even after filtering, it is strongly dependent on amplitude variations, presenting abrupt alterations when moving from high to modest amplitude values. The dependence of natural frequencies on signal amplitude is a clear indication of non-linear structural behavior (Martinelli et al. 2009). In particular, changes due to amplitude variations are also higher than those due to the entry into a different damage scenario. This fact makes instantaneous frequency unusable as the only parameter for damage identification purposes.

In order to apply the procedure proposed in Section 2, a computational algorithm was written simulating online processing, and therefore using a small subset of data at a time (consisting of 2000 couples of frequency-amplitude parameters), which is updated as reported in Section 2.1, at 10 seconds intervals (replacing therefore 1000 couples of values at a time with new incoming identified parameters).

In Figures 5-8, the frequency-amplitude data referred to the first modal response evaluated at the 7th floor of the test structure is reported over time (represented as a color bar next to each figure). In these diagrams, the couples of parameters are represented as dots in the frequency-amplitude plane and the values referred to the same τ-th updating step are plotted with the same color.

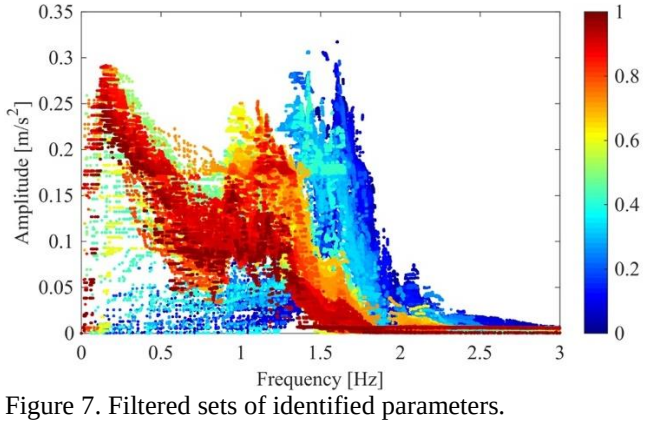

Figure 7. Filtered sets of identified parameters.

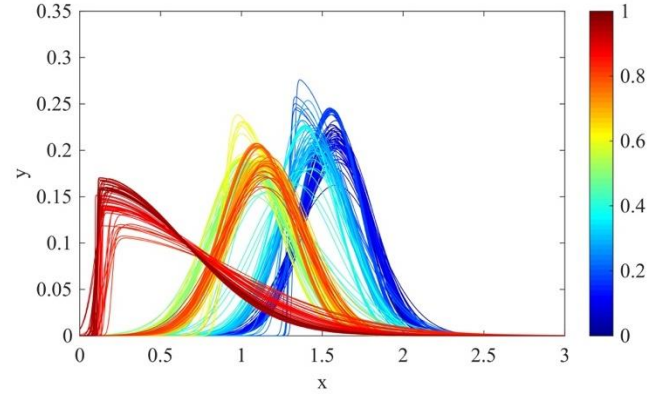

Figure 8. Models identified from filtered data.

The total time duration of 3300s is normalized to the interval 0-1 in the color bar of these figures. In Figure 5, the data is represented as it is extracted, i.e., without any selection criterion. It is possible to observe that some time intervals corresponding to the ambient vibration data sets are only characterized by low-amplitude values. In these parts, the model fitting would be based on a restricted range of amplitudes and would thus not be representative of the actual structural behavior. In Figure 6, the selection criterion proposed in this paper is applied and, indeed, each data set $(\varphi_\tau, \psi_\tau)[n]$ is composed of samples characterized by a wide set of amplitudes. In Figure 7, amplitude-based data sorting is performed and a median filter of 51 samples is applied, obtaining a $(\varphi_\tau, \bar{\psi}_\tau)[n]$ data set at instant τ. This step is done in order to de-noise the frequency-amplitude distribution and to prepare it for model fitting. In Figure 8, the model described in Equation 2 is reported, fitted to the data windows illustrated in Figure 7. It is possible to observe that the maximum value of these distributions is a damage-sensitive feature, since it shifts in the frequency axis as the damage scenario changes.

In Figure 9, the mean, variance and skewness of the models identified at the 7th floor of the test structure are reported, together with the DSF proposed in Equation 7. It is observable that the mean is sensitive to damage and insensitive to amplitude variations. Variance and skewness indicate the spread and asymmetry of the distribution, and are therefore linked to the non-linearity (Sun et al. 2014). As concerns variance, the identified value grows following the structural progressive damage, not depending on the amplitude level, while skewness shows a sharp increase in the last scenario, when the damage level is maximum. In each damage scenario, the DSF is quite a constant, except for a transition interval at the beginning of each scenario, which is related to the updating of data sequences.

In Figure 10 the variation of DSF evaluated at each level of the specimen is reported, while in Figure 11 the cumulative amount of detected "positives" is plotted over time.

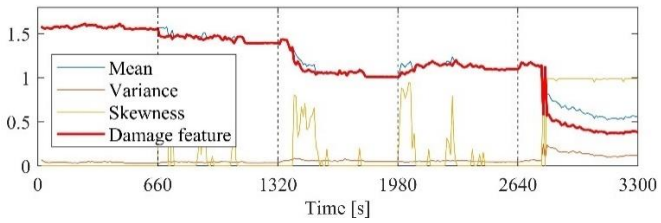

Figure 9. Parameters identified from model fitting.

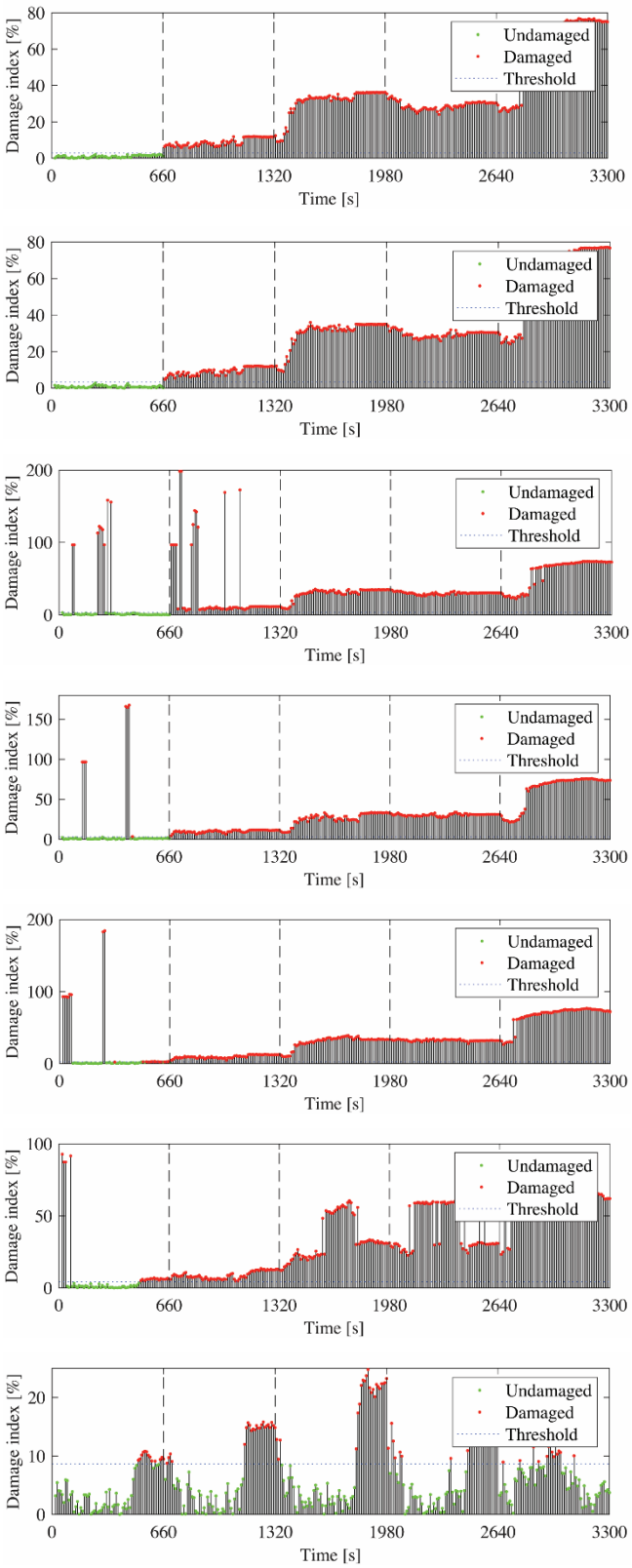

Figure 10. Variation of DSF evaluated at each level, from the top (level 7) to the bottom (level 1).

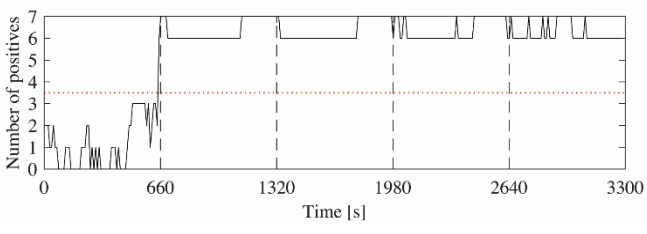

Figure 11. Cumulative number of positives detected.

In particular, the variation reported in Figure 10 is computed as the percentage variation of the DSF with respect to the median value computed over a baseline of the first 30 samples of DSF (each obtained through model fitting performed at time steps of 10 seconds). The threshold fixed for damage detection is chosen as three times the variance computed over the same baseline set, excluding the outliers (intended as the values exceeding three times the median absolute deviation).

Some spurious results in the damage detection are observable both for the undamaged and the damaged conditions, which become more numerous at the lower levels of the specimen.

A study about the accuracy of damage detection was also conducted and, in Figure 12, the percentage amount of true/false negative/positives is reported for each damage scenario and each level of the test structure. In particular, by analysing the data collected at the top floors, damage detection is more accurate, as for levels 6 and 7 (indicated in the figure as LV6 and LV7 respectively) the 100% of tests performed in the undamaged scenario have resulted as “negative” and the 100% of the tests performed in all the damage scenarios have resulted as “positive”. On the other hand, from level 2 to 5, the positives are correctly detected at 100%, while some “false positive” values are identified in the undamaged scenario. At level 1, a considerable percentage of “false negatives” was detected, making the estimation unreliable. This fact is due to the low amplitude level of the structural response collected at the lower floors, which is mostly affected by noise. However, analysing the results from all levels, as performed in Figure 11, a correct damage detection can be achieved for all scenarios, setting 50% of “positives” as a threshold.

Following a centralized initial procedure for the construction of the analysis filter, the possibility of evaluating the DSF individually at each level allows a considerable advantage for the energy efficiency aspect, as the level of wireless data transmission can be minimized and may only consist of a "positive" signal transmitted when the DSF exceeds the selected threshold. When a large number of positives are collected from a central monitoring base, the probability that the structure is actually damaged increases, making necessary more accurate analyses aimed at damage localization and at determining the causes of the variation registered in dynamic behaviour.

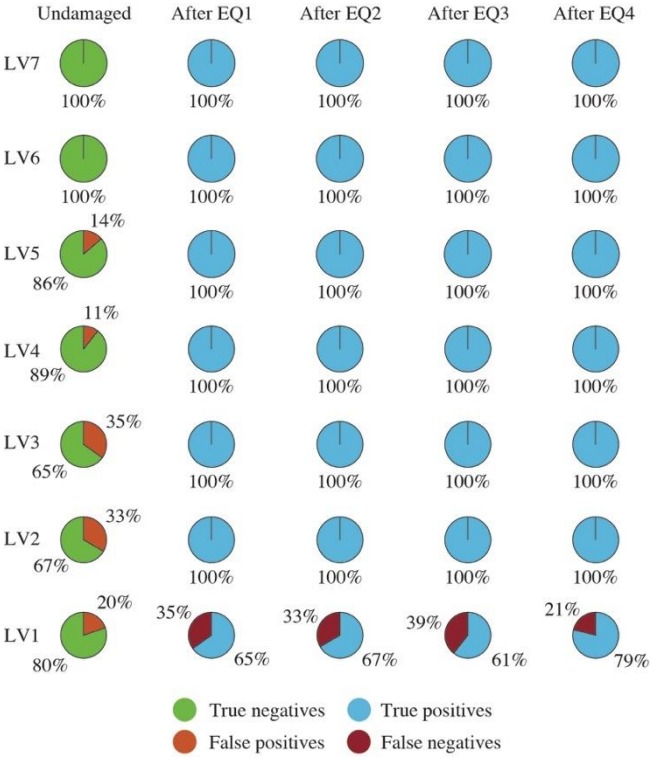

Figure 12. Results of damage detection for each scenario.

4 CONCLUSIONS

In this paper, an algorithm is presented aimed at the selection of instantaneous parameters in order to compute a DSF which is independent of the variations in excitation amplitude.

The proposed method was tested on a set of data composed of signals recorded on a structure with non-linear behaviour in different damage scenarios and environmental conditions, in order to evaluate the effectiveness of the DSF in tracking the ongoing damage in real time without showing detection errors when the excitation amplitude changes.

The identification results proved to be particularly accurate and, for most cases, are not related to variations in the excitation amplitude. Moreover, the accuracy is higher for sensors placed at the upper levels of the specimen, showing some spurious terms at the lower levels.

However, in order to increase the level of robustness of the identification procedure, all the nodes were considered, showing how the cumulative number of positives identified in real time is a reliable damage index that involves an extremely reduced wireless transmission rate.

In this way, the energy efficiency of the entire monitoring system is optimized and the proposed solution can be implemented by means of low-cost technologies, making this method suitable for early detection of damage even for minor structures.

REFERENCES

Azzalini, A., 2013. *The skew-normal and related families*, Cambridge University Press.

Bazzucchi, F., Restuccia L., Ferro, G.A., 2018. Considerations over the Italian road bridge infrastructure safety after the Polcevera viaduct collapse: past errors and future perspectives, *Fracture and Structural Integrity*, **46**, 400-421.

Billings, S.A., 2013. *Nonlinear system identification: NARMAX methods in the time, frequency, and spatio-temporal domains*, Wiley.

Brincker, R., Ventura, C.E., 2015. *Introduction to operational modal analysis*, John Wiley & Sons.

Cardoso, R.A., Cury, A., Barbosa, F., Gentile, C., 2019. Unsupervised real-time SHM technique based on novelty indexes, *Structural Control and Health Monitoring*, **26**, e2364.

Gentile, C., Ruccolo, A., Saisi, A., 2019. Continuous dynamic monitoring to enhance the knowledge of a historic bell-tower, *International Journal of Architectural Heritage*, April 2019.

Giordano P.F., Ubertini, F., Cavalagli, N., Kita, A., Ramos, L.F., Masciotta, M.G., 2018. Diagnostic investigations and structural health state assessment of San Pietro bell tower in Perugia. *10th International Masonry Conference*. July 9 – 11, Milan, IT.

Kim, R.E., Li, J., Spencer, B.F., Nagayama, T., Mechitov, K.A., 2016. Synchronized sensing for wireless monitoring of large structures, *Smart Structures and Systems*, **18**(5), 885-909.

Kita, A., Cavalagli, N., Ubertini, F., 2019. Temperature effects on static and dynamic behavior of Consoli Palace in Gubbio, Italy, *Mechanical Systems and Signal Processing*, **120**, 180-202.

Limongelli, M.P., Spina, D., Guéguen, P., Langlais, M., Wolinieck, D., Maufroy, E., Karakostas, C.Z., Lekidis, V.A., Morfidis, K., Salonikios, T., Rovithis, E., Makra, K., Masciotta, M.G., Lourenço, P.B., 2019. S^2HM in some European countries, in: Limongelli M., Çelebi M. (eds), *Seismic Structural Health Monitoring*, Springer Tracts in Civil Engineering, Springer, Cham.

Magalhães, F., Cunha, A., Caetano, E., 2012. Vibration based structural health monitoring of an arch bridge: from automated OMA to damage detection, *Mechanical Systems and Signal Processing*, **28**, 212-228.

Martinelli, P., Filippou, F.C., 2009. Simulation of the shaking table test of a seven-story shear wall building, *Earthquake Engineering and Structural Dynamics*, **38**, 587-607.

Moaveni, B., He, X., Conte, J.P., Restrepo, J.I., 2010. Damage identification study of a seven-story full-scale building slice tested on the UCSD-NEES shake table, *Structural Safety*, **32**(5), 347-356.

Moaveni, B., He, X., Conte, J.P., Restrepo, J.I., Panagiotou, M., 2011. System identification study of a 7-story full-scale building slice tested on the UCSD-NEES shake table, *Journal of Structural Engineering*, **136**(7), 705-717.

Noel, A.B., Abdaoui, A., Elfouly, T., Ahmen, M.H., Badawy, A., Shehata, M.S., 2017. Structural health monitoring using wireless sensor networks: a comprehensive survey, *IEEE Communications Surveys & Tutorials*, **19**(3), 1403–1423.

Peeters, B., Maeck, J., De Roeck, G., 2001. Vibration-based damage detection in civil engineering: excitation sources and temperature effects, *Smart Materials and Structures*, **10**(3), 518-527.

Quqa, S., Landi, L., Diotallevi, P.P., 2019. Real time damage detection through single low-cost smart sensor. *7th ECCOMAS Thematic Conference on Computational Methods in Structural Dynamics and Earthquake Engineering*. June 24-26, Crete, GR.

Ramos, L.F., Marques, L., Lourenço, P.B., De Roeck, G., Campos-Costa, A., Roque, J., 2010. Monitoring historical masonry structures with operational modal analysis: two case studies, *Mechanical Systems and Signal Processing*, **24**(5), 1291-1305.

Saisi, A., Gentile, C., Ruccolo, A., 2018. Dynamic monitoring of ancient masonry towers: environmental effects on natural frequencies. *10th International Masonry Conference*. July 9-11, Milan, IT.

Sun, W., Li, H., Ying, L., 2014. Damping identification for the nonlinear stiffness structure, *Journal of Vibroengineering*, **16**(2), 770-780.

Tokognon, C.A., Gao, B., Tian, G.Y., Yan, Y., 2017. Structural health monitoring framework based on Internet of Things: a survey, *IEEE Internet of Things Journal*, **4**(3), 619-635.

Worden, K., Tomlinson G.R., 2001. *Nonlinearity in structural dynamics: detection, identification and modeling*, Institute of Physics Publishing Ltd.

Zonno G., Aguilar, R., Boroschek, R., Lourenço, P.B., Analysis of the long and short-term effects of temperature and humidity on the structural properties of adobe buildings using continuous monitoring, *Engineering Structures*, **196**, 109299.